Journal of Structural Geology 35 (2012) 28–39

Contents lists available at SciVerse ScienceDirect

Journal of Structural Geology

journal homepage: www.elsevier.com/locate/jsg

Flexural unfolding of horizons using paleomagnetic vectors

M.J. Ramón [a,b,*], Emilio L. Pueyo [a], José Luis Briz [c,d], Andrés Pocoví [b], José Carlos Ciria [c]

[a] Instituto Geológico y Minero de España (IGME), Unidad de Zaragoza, Zaragoza, Spain
[b] Departamento de Ciencias de la Tierra, University of Zaragoza, Spain
[c] Departamento de Informática e Ingeniería de Sistemas, University of Zaragoza, Spain
[d] I3A Research Institute, University of Zaragoza, Spain

ARTICLE INFO

Article history:
Received 19 May 2011
Received in revised form
18 November 2011
Accepted 25 November 2011
Available online 3 December 2011

Keywords:
Structural restoration
Paleomagnetism
Developable surfaces
Internal deformation
Analog models

ABSTRACT

This paper introduces a new restoration method (*Pmag3Drest*) designed for complex folded structures (non-cylindrical, non-coaxial). It combines paleomagnetic vectors and bedding markers setting up a reference system that allows deformed and undeformed surfaces to be related to one another. We assume flexural conditions during the deformation. Consequently, the stratigraphic horizons are considered to be *globally developable* surfaces with total area preservation except in specific deformation areas. Using paleomagnetism in the proposed restoration process (*Pmag3Drest*) helps to locate these areas with greater accuracy. It is similar to other approaches based on triangulations, but it forces the available paleomagnetic data to converge with the paleomagnetic reference vector during the restoration process. Our experiments use computer and analog models in which the deformed and undeformed surfaces are perfectly known. This enables us to apply the restoration method to the deformed surface and compare the parameters of the restored surface with those of the initial undeformed surface to quantify the quality of the method. Paleomagnetic data anchor the surface leading to more accurate results.

1. Introduction: restoration of flexural folds

Three-dimensional reconstructions of the subsurface entail the integration of discrete and heterogeneous datasets and are an important field in Earth Sciences due to their considerable socio-economic implications. Methodological and technological developments over the last two decades have resulted in a wide variety of methods, tools and software packages (e.g., *Move* by Midland Valley Exploration [Griffiths et al., 2002], *gOcad* and *Kine3D* [Moretti et al., 2005] by Paradigm; and *Dinel3D* by iGeoss [Maerten and Maerten, 2006]). They allow trustable georeferenced subsurface reconstructions to be performed with a reasonable level of predictability, especially when abundant surface and subsurface information is available. Problems arise when there are limited data to build 3D models or when deformation processes are complex, and for that reason, the aim of the first restoration methods, which appeared in the 1970's, was to validate subsurface reconstructions. In addition, restoration tools may also be useful to predict deformation patterns. Restoration techniques can be geometrical (as explained latter) or geomechanical (Moretti et al., 2005; Muron, 2005; Maerten and Maerten, 2006; Moretti, 2008; Durand-Riard et al., 2010). We focus on geometrical approaches as geomechanical methods require more assumptions and a better knowledge of the subsurface geology (petrophysics, etc).

Geometrical restoration algorithms can be divided into different approaches as a function of the number of dimensions considered: *cross-section* or *map-view* (2D), *surface* (2.5D) and *volume* (3D) *restoration*. At regional scales and crustal levels, we can assume that deformation does not change the total rock volume, at least overall (Goguel, 1952). These methods are, therefore, mostly based on the preservation of lengths, angles, areas and/or volumes, as well as the minimization of strain. These principles were first applied in 2D leading to the techniques of cross-section balancing (Dalhstrom, 1969; Elliott, 1976; Hossack, 1979; Cooper, 1983) and map-view restoration (Rouby et al., 1993; Arriagada et al., 2008). Over the last twenty years, the original 2D restoration techniques have been extended to 3D, starting with surface methods like that of Gratier et al. (1991) usually considered to be 2.5D. Surface restoration methods are based on the restoration of individual horizons to the horizontal and are usually extended to multi-surface restoration by assuming that the thickness of the layers is constant or varies in a controlled way (Williams et al., 1997).

* Corresponding author. Instituto Geológico y Minero de España (IGME), Unidad de Zaragoza, Zaragoza, Spain.
E-mail address: mj.ramon.ortiga@gmail.com (M.J. Ramón).

0191-8141/$ – see front matter © 2011 Elsevier Ltd. All rights reserved.
doi:10.1016/j.jsg.2011.11.015

For surface restoration, Rouby et al. (2000) break the process down into two separate steps: *unfolding* and *unfaulting*. In turn, unfolding algorithms are based on two deformation mechanisms: *simple shear* (Kerr et al., 1993; Buddin et al., 1997) and *flexural slip* (Gratier et al., 1991; Gratier and Guillier, 1993; Williams et al., 1997; Léger et al., 1997; Griffiths et al., 2002; Thibert et al., 2005). Simple shear assumes folds have internal deformation, whereas flexural slip assumes surfaces are globally developable (area and length preserved). The unfaulting step involves dividing the region into rigid horizontal blocks bounded by faults (Audibert, 1991; Rouby et al., 1993; Arriagada, 2004; Arriagada et al., 2008). Using finite elements (Dunbar and Cook, 2003) or by parameterizing the surface (Leger et al., 1997; Massot, 2002), 2.5D restoration can also be performed in one step.

In all these methods, the bedding plane is the basic reference for relating the deformed to the undeformed surfaces. The problem is that the bedding plane cannot be used as a three-dimensional reference system, because it is defined by a single vector and additional constraints are required. This is particularly important when dealing with complex structures, such as non-cylindrical structures and the superposition of non-coaxial geometries, which are responsible for the so-called *out-of-plane motion* in the classic 2D approaches. In this context, paleomagnetism can contribute to building a more complete reference system and reducing the uncertainty in restoration processes. The deformed and undeformed surfaces can be related by means of the basic deformation mechanisms (Ramsay, 1967; Cobbold and Percevault, 1983; Ramsay and Hubbert, 1983): internal deformation, translation and rotation (Fig. 1). Since magnetization behaves as a passive marker during the deformation processes, it provides us with information on one of the variables, namely the rotation.

Accordingly, the combination of the paleomagnetic vector and the bedding plane is a good reference that can be very useful in restoration techniques, since both are known accurately in the deformed and the undeformed surfaces. The use of paleomagnetism in restoration tools was recommended in the early 1990's (McCaig and McClelland, 1992). So far, however, relatively few researchers have tried using paleomagnetic information to double-check the rotation inferred from restoration methods (Bonhommet et al., 1981; Bourgeois et al., 1997; Arriagada, 2004). Recently Arriagada et al. (2008) have modified the map-view restoration method, developed by Audibert (1991) and Rouby et al. (1993), to include paleomagnetic data as primary information. Although their approach is the first we are aware of that incorporates paleomagnetic data, it is still a 2D restoration method, as are two map-view methods that have been proposed involving paleomagnetic vectors (Millán, 1996, 2006; Pueyo, 2000, 2004). These map-view methods, which correct shortening estimates from cross-sections and calculate realistic shortening, have recently been applied in the Pyrenees (Oliva and Pueyo, 2007) and in the Rocky Mountains (Sussman et al., 2011).

In this paper, we introduce the first surface restoration method that uses paleomagnetic vectors as a primary reference. The starting point is the UNFOLD method developed by Gratier et al. (1991) and by Gratier and Guillier (1993), as it is a simple geometric approach into which paleomagnetic variables can be easily incorporated and it is valid for non-cylindrical structures. We assess the accuracy of the restoration algorithm using computer and analog models. These allow us to set up a known initial undeformed surface (a horizontal horizon). We then perform a forward deformation to obtain a controlled deformed surface. Subsequently, we apply a restoration method to that deformed surface, and compare the result from the restored state with the initial undeformed surface. With an ideal restoration method the two states should match perfectly and, therefore, we can quantify the quality of the restoration by measuring the differences between them. This approach is a valuable complement to other ways of assessing the accuracy and results of a restoration, like those based on well data, fracture distribution or kinematic models (Guzofski et al., 2009).

2. Restoration with paleomagnetism: the method

As in any restoration method, we need to establish some reasonable initial assumptions. We assume that:

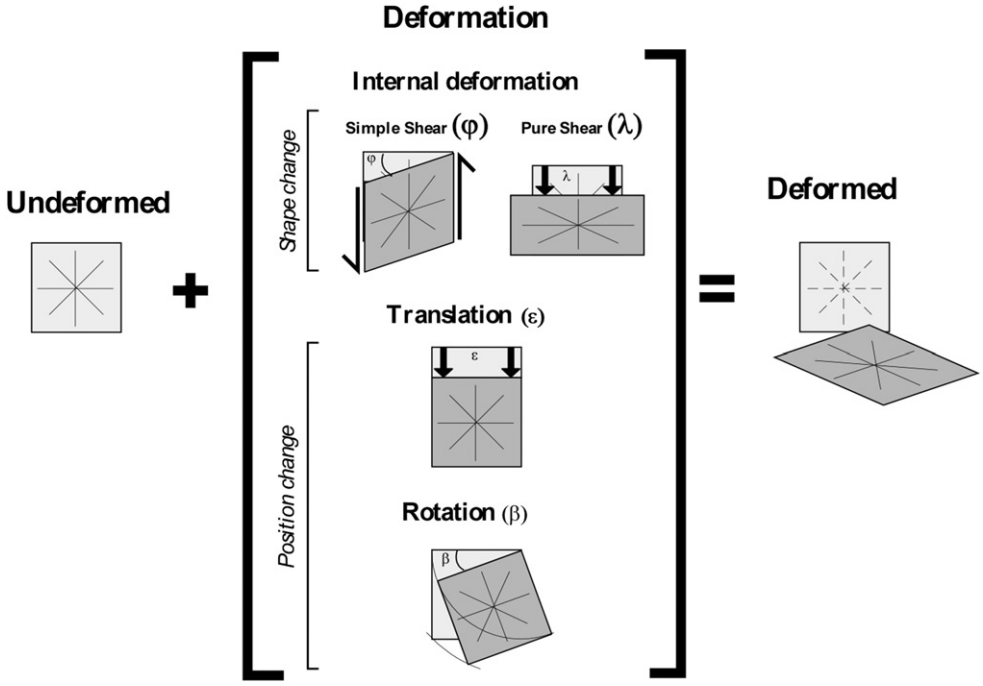

Fig. 1. Basic deformation mechanisms (internal deformation, translation and rotation) are able to relate the deformed and undeformed surfaces if the correct (non-commutative) sequence of processes is applied.

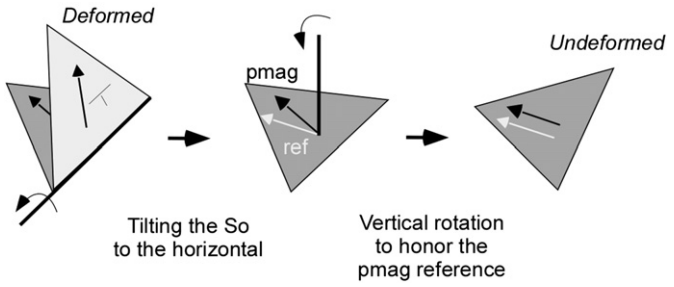

Fig. 2. The concept: paleomagnetism as an additional tool in restoration methods. The surface is rotated to the horizontal with the bedding plane and then it is rotated around its vertical axis to fit with its paleomagnetic reference vector.

1. Layers are horizontal in the undeformed surface; horizontality is the basic assumption in all restoration methods.
2. The folded surface is *developable*; it has been transformed by preserving angles, lengths and areas, so the Gaussian curvature is constant and zero. The method is also valid for *globally developable surfaces*, like those derived from rock volumes that have undergone flexural folding as described by Ramsay (1967), i.e., flexural flow on the flanks or tangential-longitudinal strain at the hinges.
3. An even distribution of paleomagnetic vectors characterizes the folded surface. These vectors are primary (recorded at the time of deposition) and behave as passive markers during the deformation. Both the local and the paleomagnetic reference vectors have to be reliable in the sense used by Van der Voo (1990) and Pueyo (2010).

\The UNFOLD method, like most flexural restoration tools, requires the first two of these assumptions, and the paleomagnetic restrictions can be easily integrated. The horizon is defined as a mesh of triangular elements that are first laid flat, and then rearranged (translated and rotated) to minimize distances between neighbors. The main change on adding paleomagnetic data is that the rotation is not free when minimizing the distances, as it is constrained by the paleomagnetic reference vector (Fig. 2). The software (*Pmag3Drest*) has been developed using *Matlab* (www.mathworks.com).

The method involves the following sequence of eight steps (Fig. 3):

1. Surface definition. A set of points with Cartesian coordinates describes the folded surface and determines the nodes of the rigid triangular elements of the mesh. To build the mesh, Delaunay (1934) or regular triangulation (Hjelle and Dæhlen, 2006) can be used.
2. Incorporation of paleomagnetism. The method adds paleomagnetic vectors in triangular elements where paleomagnetic data are available, only considering the magnetic declination (the so-called "horizontal component"). The vector passes through the barycentre of the triangle (Fig. 4). The accuracy of the data, α_{95} (Fisher, 1953), can be related to the local paleomagnetic vector. In the case of sparse or poorly distributed vectors, it is possible to extrapolate this paleomagnetic vector using *dip-azimuth domains* (similar to the *dip-domain* concept of Suppe, 1985 and Fernández et al., 2003), which effectively means that all the triangles with similar stratigraphic orientation (i.e., those in the same bedding plane) will have the same paleomagnetic vector.
3. Flattening. Each triangle is automatically laid flat to form a horizontal surface, by horizontal rotation about its strike axis. In the case of overturned beds, we treat the *stratigraphic polarity* as a vector in each element.
* Pin-line definition. The barycentre of these elements is in the same position in the deformed and undeformed surfaces. As in cross-section balancing, it is the point (or line) that anchors the surface. Restoration is highly dependent on the *pin-line*, which must therefore be carefully chosen with geological criteria (i.e., undeformed foreland).
4. Vertical-axis rotation. The paleomagnetic vectors from the pin-line elements must converge with the paleomagnetic reference vector. Significant rotations are very unlikely since the pin-line should be chosen in stable (undeformed) portions of the horizon. If, however, there are substantial rotations, we apply an equal rigid-body rotation to the horizon at this stage.
5. Translation and rotation. Each triangle is translated and rotated in order to fit with its neighbors using the method of least-squares. We minimize distances between shared vertices, bearing in mind the paleomagnetic reference. This step starts at the *pin-line* (or *pin-point* for single triangles). If an element has paleomagnetic data, the related rotation is constrained by the paleomagnetic vector (Fig. 4), with a number of degrees of freedom that is determined by the α_{95} value. If the initial (undeformed) surface were completely developable (without any deformation), the restoration process would end at this step.
6. Iterating. The translation and rotation process is iterated a certain number of times, or for as long as the total distance error remains below a threshold, $e = \sum D / \sum M$. In this expression, e is the error, D the sum of distances between the vertices of each triangle and the triangular hole defined by its neighbors and M the sum of the medians of each triangle (Fig. 4). This step is especially important in the original UNFOLD method, where paleomagnetism is not considered (Gratier et al., 1991) and rotation is free.
7. Welding. After the iterative translation and rotation, the surface becomes discontinuous, with holes and overlaps, assuming that the deformed surface that has been restored was not completely developable. In order to obtain a continuous surface, this step involves joining or "welding" the shared vertices of neighboring triangles through an average value, allowing internal deformation to take place.
8. Optimization process. This step is only performed when the restoration uses paleomagnetic data. At this point of the restoration process, the maximum paleomagnetic error (the difference between the local and the reference paleomagnetic vectors) is less than the α_{95} angle, and we may want to sacrifice accuracy in favor of preserving area. The vertices of the triangles are randomly modified to minimize a potential function (Eq. (1)), following the simulated annealing method (Kirkpatrick et al., 1983; Press et al., 1992). The potential function (U) includes the paleomagnetic error ($1\text{-}\cos[ref\text{-}pmag_i]$) and the internal deformation (dilation in terms of variation in area described by Eq. (2)) with specific weights for each term (A and B).

$$U = A\sum_i [1 - \cos(ref - pmag_i)] + B\sum_i \left(\frac{\text{area}_{0i} - \text{area}_i}{\text{area}_i}\right) \qquad (1)$$

We have used three parameters to describe and quantify the restoration results. The dilation and the deformation ellipse enable us to compare the deformed and undeformed surfaces. Theoretical or expected values are calculated comparing the initial undeformed surface with the deformed surface, while estimated values are calculated by comparing the restored surface with the deformed surface. In an ideal case, theoretical and estimated parameters should match. The shape coefficient relates the initial surface with the restored surface.

1. Dilation. This is a measure of the variation in the area of the triangles (Eq. (2)). Negative or positive dilation respectively correspond to contraction or expansion of the folded surface (deformed surface), with respect to the restored surface (which ideally matches the initial undeformed surface).

$$\text{Dilation} = \frac{\text{Area}_{\text{folded}} - \text{Area}_{\text{restored}}}{\text{Area}_{\text{restored}}} \quad (2)$$

2. Deformation ellipse. This is a measure of the anisotropy of the deformation. First, we compute the affine transformation matrix

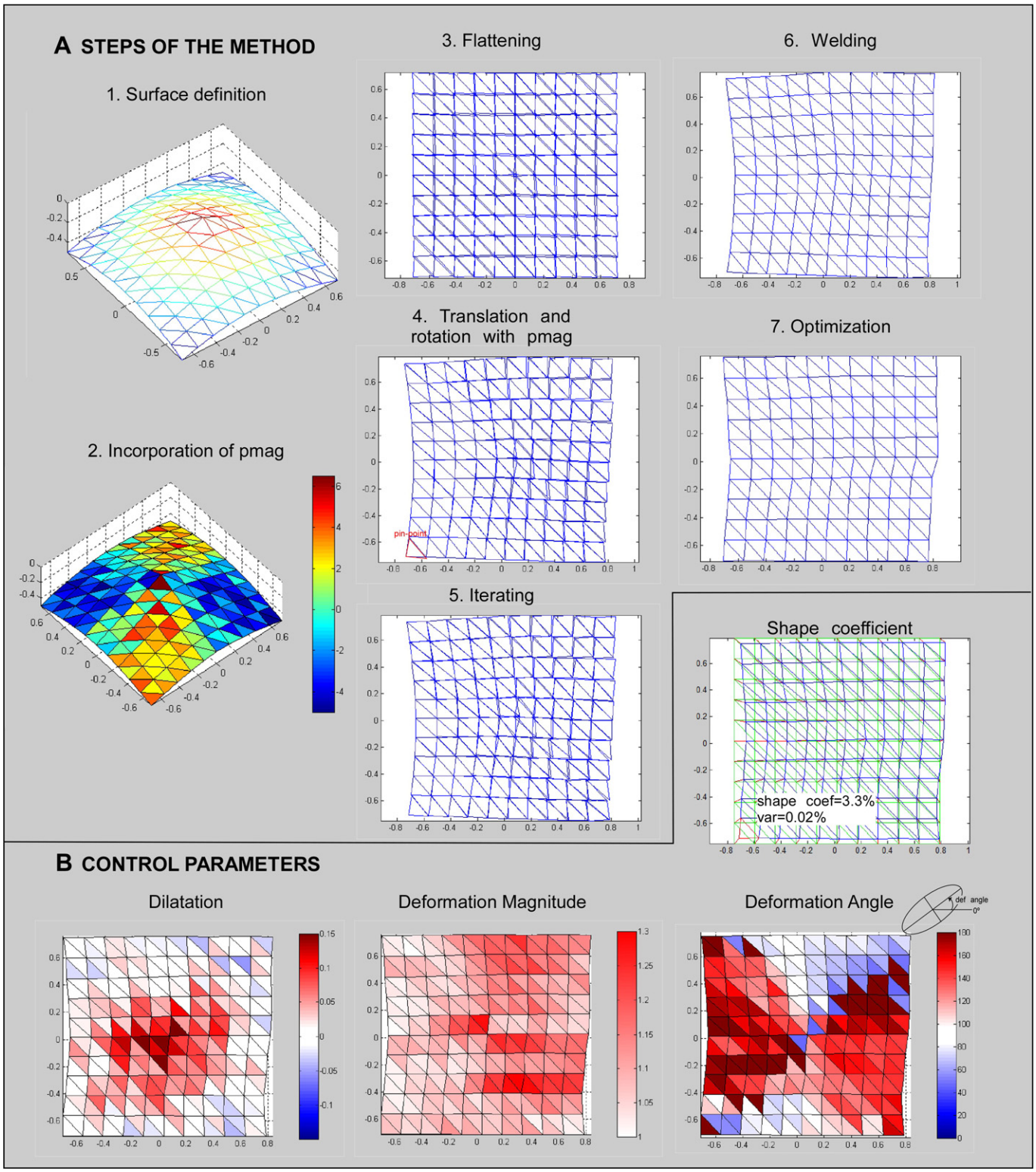

Fig. 3. A) The method, step by step. B) Control parameters: shape coefficient and variance (percentage), dilation and ellipse of deformation (magnitude and angle).

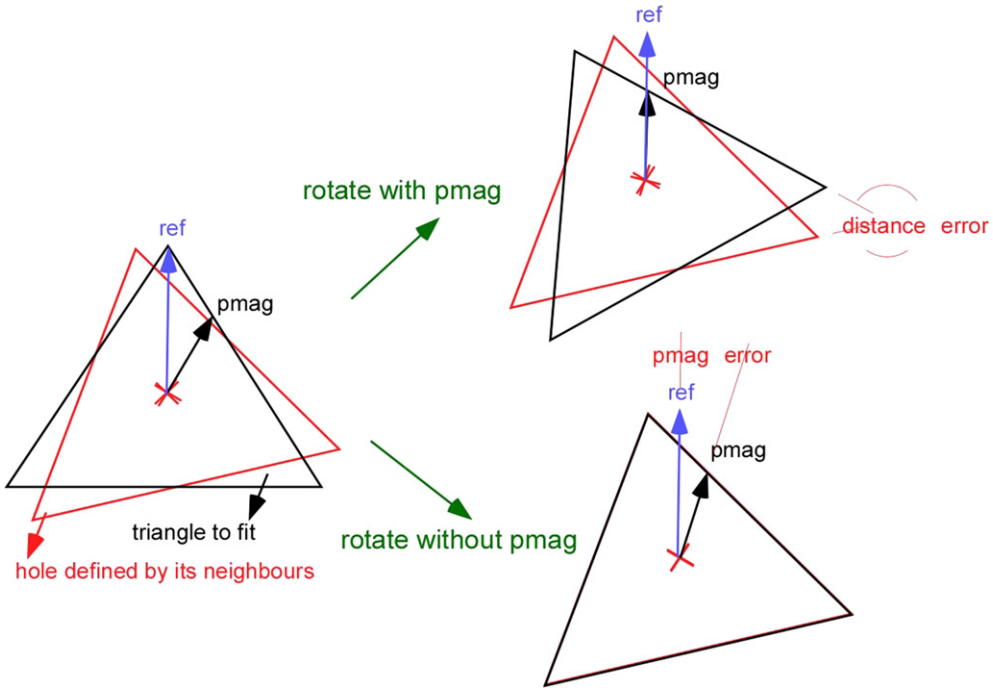

Fig. 4. Rotation of an individual triangle with and without using the paleomagnetic vector. *G* is the barycentre of the triangle. Pmag is the paleomagnetic vector and ref its reference. D_i is the distance between common vertices.

M that relates the points in the two states. The matrix coefficients are determined using the coordinates of the vertices of the folded and restored surfaces. Second, we consider a circle centered on the barycentre of each triangle in the restored state, and apply the transformation matrix *M* to the canonical matrix of the circle. The circles become deformation ellipses. The magnitude of the deformation is then calculated as the ratio between the major and minor axis of the deformation ellipse, while the orientation of the deformation is the angle between a horizontal axis and the major axis of the ellipse (Eq. (3)).

$$\begin{aligned} Def\_\text{magnitude} &= \text{majAxis}/\text{minAxis} \\ Def\_\text{angle} &= \alpha_{\text{majAxis}} \end{aligned} \tag{3}$$

3. Shape coefficient. This is a measure of the difference in shape between the restored and the initial undeformed surfaces reflecting the distance between all single points. The shape coefficient is the mean value of the distances divided by the maximum length of the surface (Eq. (4)). We also calculate its variance (Eq. (5)).

$$\text{shapeCoeff} = \sum \text{dist}/N \cdot \text{length} \tag{4}$$

$$\text{var} = \sum (\text{dist} - \text{meanDist})^2/N \cdot \text{length} \tag{5}$$

3. Discussion

To validate the restoration tool and to assess the goodness of fit of the results we use computer and analog models. In contrast to natural examples, for which information is usually sparse and inhomogeneous, in these models the initial undeformed and deformed surfaces are both known. A perfect restoration method should yield the initial undeformed surface. Therefore, we can quantify the accuracy of any restoration method by estimating how much the restored state differs from the initial undeformed surface, known from the outset.

3.1. Example of a computer model: deformed cone

We first define a preliminary deformed surface consisting of a developable cone using *Matlab*. Since this deformed surface (the developable cone) shows no deformation with respect to the initial undeformed surface (a horizontal horizon), the cone can be unfolded using the restoration method without adding strain. We add the paleomagnetic reference to each triangular element in the initial undeformed surface (horizontal) and calculate its position in the preliminary deformed surface according to the proper (forward) deformation that maps the horizontal horizon to the developable cone. Second, we deform that preliminary deformed surface (the developable cone with paleomagnetism) using geological 3D reconstruction software (*gOcad*). To deform the cone, the vertices of the triangles that form the hinge are moved up an arbitrary distance. The paleomagnetic vectors are recalculated accordingly; that is, they behave as passive markers recording the deformation. Lastly, this final deformed surface (which is now undevelopable) is restored with the new method (*Pmag3Drest*) with and without using the paleomagnetic information (Fig. 5).

The theoretical (or expected) control parameters we use to evaluate the restoration are calculated by comparing the initial undeformed surface (which matches the surface we obtain by restoring the developable cone) with the final deformed surface (the undevelopable cone with hinge deformation) (Fig. 5B). The developable cone was deformed randomly; that is, we deliberately did not attempt to model a specific geological process, so that we would not expect any preferential deformation orientation. As the dilation and deformation ellipses provide similar information, we only plot dilation to indicate the quality of further restorations.

The estimated control parameters are calculated by comparing the restored surface with the deformed cone (Fig. 5C). In this example, the final shape of all the restored surfaces is fairly similar, regardless of whether we use the paleomagnetic information. On the other hand, the surface restored without paleomagnetic data does not indicate any internal deformation (dilation) in the triangular elements, while the surface restored with consideration of paleomagnetism shows relatively large dilation values approximately along the hinge area, where that kind of deformation can be expected. Unlike the UNFOLD method, the use of paleomagnetic data in this case helps to properly anchor the restored surface and locate the internal deformation.

At this point, we can apply an optimization process to the former result. The optimization algorithm tends to distribute the error across the entire surface. It is useful to obtain a smoother surface, when we are able to ensure there is no deformation. On the other hand, it is better to omit this last step when we are trying to identify a possible deformation, as it causes the model to lose information, the deformation always becoming weaker after the optimization.

In the former example, we assumed that the paleomagnetic vectors were completely accurate. In a real case, the paleomagnetic vectors will always have a degree of error, described by a 95% confidence cone (α_{95}). Now, we examine the result for the case where we consider a realistic set of paleomagnetic vectors (Fig. 6A). We have added a random angular deviation of $\pm5^\circ$ and $\pm10^\circ$ to the definition of the paleomagnetic data to be used for the restoration. As a result, the strain distribution in the corresponding restored surfaces is less certain than in the first case ($\alpha_{95} = 0^\circ$). Nevertheless, when the angular deviation of paleomagnetic data is small ($\alpha_{95} = 5^\circ$), the restored surface still helps to locate areas of maximum deformation.

In the examples considered so far, the paleomagnetic vectors have been defined in all triangular elements of the surface. In nature, the paleomagnetic field can only be measured in outcrops. The next simulation approximates this situation (Fig. 6B). We define paleomagnetic sites at the intersection of the cone with an arbitrary topography (a horizontal plane). The paleomagnetic vectors have been extrapolated in dip-azimuth domains, so that regions with variation in the bedding plane of less than 5° have the same orientation of paleomagnetic vector. In addition, we assume that we know the paleomagnetic data in the pin-line to have a coherent dataset. When the paleomagnetic vector is accurately defined ($\alpha_{95} = 0^\circ$), it is still possible to identify the expected internal deformation at the hinge of the cone, in spite of the fact that the accuracy is lower than in the other simulations. In contrast, when there is a paleomagnetic error ($\alpha_{95} = 5^\circ$) the model shows greater inconsistencies. This underlines the fact that, although it is a time-consuming and difficult task, it is very important to obtain a large, reliable and evenly distributed set of paleomagnetic sites along any structure to be studied.

3.2. Example of analog model: conical fold

Computer models give us absolute control over the deformation process, and do enable us to analyze perfectly defined deformed and undeformed surfaces. Nevertheless, our final target is to obtain as close as possible an approximation to the initial undeformed horizon of real folded geological structures, and this is totally unknown. Analog geological models enable us to take the process of validation of a restoration method one step further. They share with real natural structures the inaccuracies introduced by digitalization, but, on the other hand, in these models we have considerable control over the deformation process and we know both the deformed and undeformed surfaces.

3.2.1. Natural example: geological setting

The analog model we describe here is based on a natural complex-structure in the southwestern Pyrenees. The Santo Domingo anticline, in the western External Sierras (Fig. 7), strikes WNW-ESE and is detached along the incompetent middle and upper Triassic levels (Nichols, 1984, 1987; Turner, 1990; Millán, 1996, 2006). Its geometry can be approximated as a conical fold with an elliptical cross-section describing parallel near-vertical limbs (Millán et al., 1995). The Santo Domingo anticline was active during the Late Oligocene-Early Miocene, during the last stage of the structural evolution of South Pyrenean sole thrust, as attested by syntectonic sedimentation along the southern flank of the fold (Puigdefàbregas, 1975; Arenas et al., 2001). The pre-continental sequence involved in the Santo Domingo anticline describes a pericline at its westernmost end (San Marzal) that runs NW and plunges an angle of 60–70° (Nichols, 1984; Pueyo, 1994 and this work). The subsurface geometry of the fold reflects a rapid decrease in the angle of the plunge of the axis westwards (Oliva, 2000; Oliva et al., 1996, 2011).

The interest of this conical structure lies in the large rotations believed to be responsible for its genesis, as originally proposed by simple analog modeling (Millán et al., 1992). Pueyo (2000) and Pueyo et al. (2003) explored this hypothesis by performing paleomagnetic analysis on both flanks of the anticline as well as on the pericline. There is a significant clockwise rotation (CW $\approx 45^\circ$) in the northern flank and almost 20° of counter clockwise rotation (CCW) in the southern flank that must gradually disappear in the non-rotated foreland (Fig. 7). A gradual rotation magnitude is observed around the fold hinge (San Marzal area). This complex geometry has arisen due to the combination of two mechanisms: 1) general along-strike variations in the magnitude of shortening associated with the diachronous emplacement of the External Sierras thrust system (Nichols, 1984; McElroy, 1990; Millan, 1996, 2006; Pueyo et al., 2004) responsible for $\approx 30^\circ$ CW rotation; and 2) the lateral disappearance of the detachment level (*Keuper* facies) to the West, as demonstrated by the borehole records (Aoiz, Roncal and Sangüesa wells; Lanaja, 1987). This latter process would have produced a pinning effect and the striking conical geometry of the fold.

3.2.2. Analog model: reconstruction

The model attempts to reproduce five main structural features: 1) the San Marzal orientation: trends 305° and plunges 67°; 2) an approximately 50° clockwise rotation in the northern flank; 3) pseudo-parallel flanks in the Sto. Domingo anticline; 4) synclines trending 305° and horizontal; and 5) the southern flank is assumed to be in structural continuity with the Ebro foreland basin and it will be used as the pin-line.

The material selected to build the model was an EVA (ethylene vinyl acetate) plate because it behaves like a *globally developable* surface (mostly developable, which allows local deformations). The thickness of the plate (0.3 cm) is proportional to the Guara Formation (see cross-section at Fig. 7B). The air within the anticline core represents the pre-Guara formations including the Triassic evaporites. The paleomagnetic vectors (declination component) are featured as lines printed on the EVA surface. A rectangular grid screen-printed on the surface provides two possible references. This 20×20 grid is composed of rectangles of 1.5×2 cm. The goal of the reconstruction process is to digitalize the nodes of the mesh defined by the two sets of lines printed on the EVA surface.

For this digitalization of the analog model we use photogrammetry. This is a simple image-based modeling technique used in many fields (for instance Fischer and Keating, 2004; among others). Pictures are taken of the model from various different angles and the software *PhotoModeler* (www.photomodeler.com) is then used to carry out a 3D reconstruction (Fig. 8).

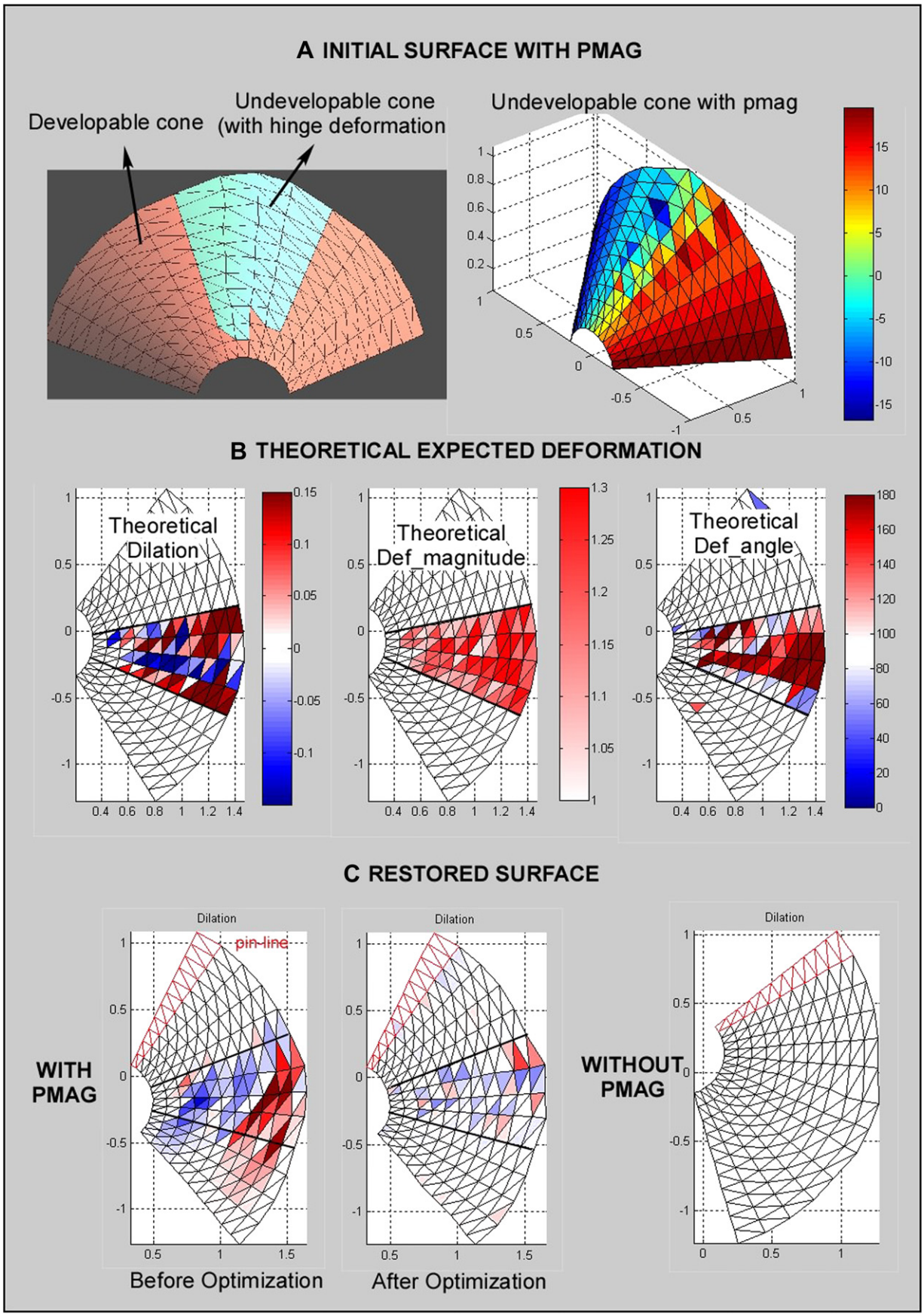
A INITIAL SURFACE WITH PMAG
Developable cone
Undevelopable cone (with hinge deformation
Undevelopable cone with pmag
B THEORETICAL EXPECTED DEFORMATION
Theoretical Dilation
Theoretical Def_magnitude
Theoretical Def_angle
C RESTORED SURFACE
WITH PMAG
WITHOUT PMAG
Dilation
pin-line
Before Optimization
After Optimization

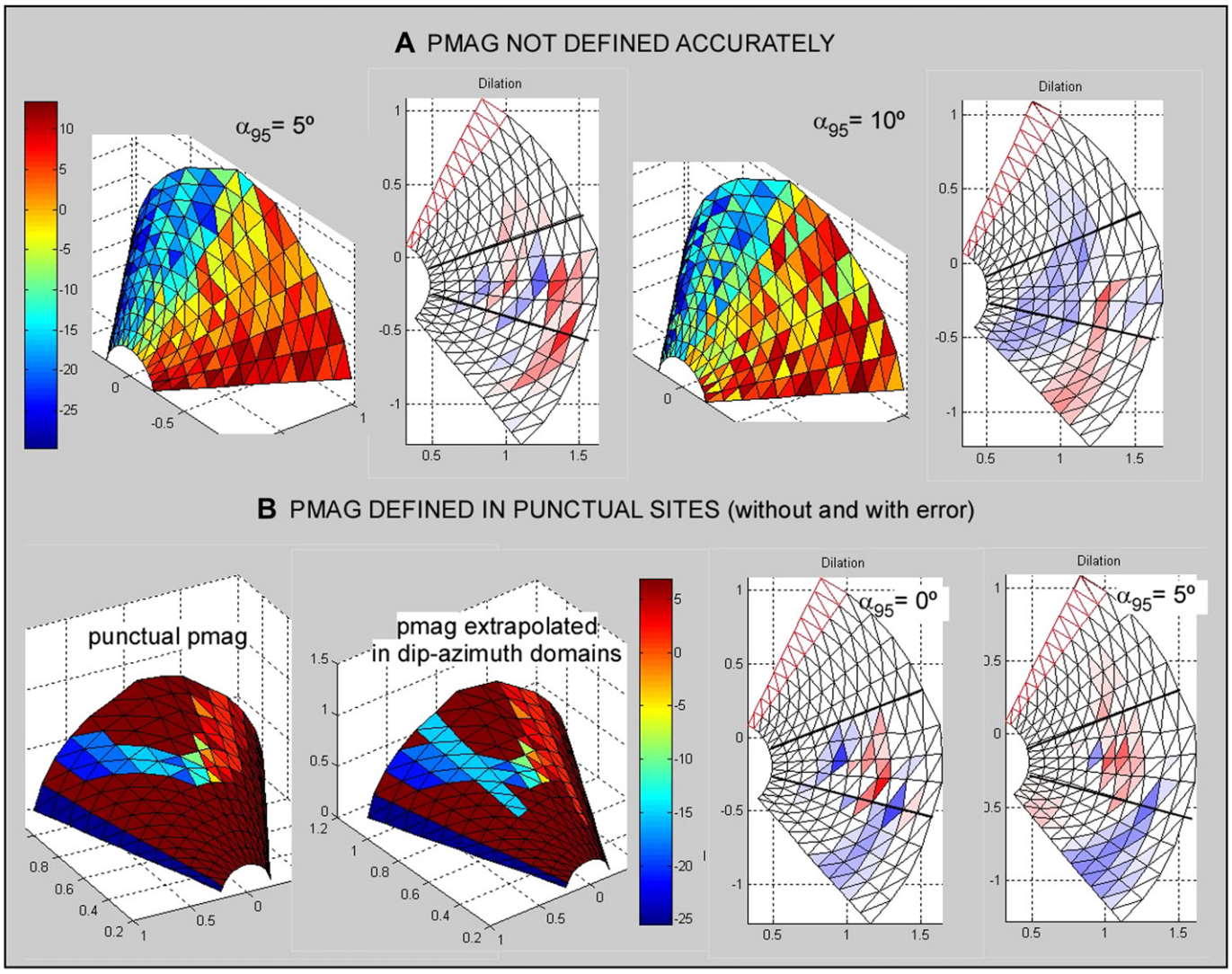

Fig. 6. Undevelopable cone. A) Restoration when the paleomagnetic vectors are defined with variable confidence angles; $\alpha_{95} = 5°$ and $\alpha_{95} = 10°$. B) Restoration when paleomagnetic vectors are defined only in limited portions of the deformed surface. We have considered perfectly defined vectors ($\alpha_{95} = 0°$) and vectors with some degree of error ($\alpha_{95} = 5°$).

3.2.3. *Analog model: restoration*

We have performed several restoration simulations using the two paleomagnetic datasets (meridian and parallel), as well as without considering paleomagnetism. We have also used different pin-points and pin-lines during the restorations. The optimization step was omitted to avoid the smoothing effect. We calculate the theoretical (expected) deformation by comparing the initial undeformed surface (horizontal grid) with the deformed surface (folded structure, Fig. 8). The curvature of the folded surface is obtained from the *gOcad* software and is also used for comparisons. The folded surface remains *globally developable*, and some extension is expected at the fold hinge (Fig. 9A).

The expected deformation (dilatation) is very similar to the simple curvature of the folded surface: since we are looking at the uppermost surface of the deformed plate, we observe expansion in the anticline hinge of the fold, and contraction in the synclines. This is the expected distribution in a tangential-longitudinal model (Ramsay and Hubbert, 1983) where extension is related to outer anticline hinges and contraction to the inner ones. However, the restoration method gives us additional and independent information with respect to curvature analysis. For example, the areas of maximum deformation also show a preferential orientation, namely the left syncline in the picture (northern flank in the real structure) displays a relatively large maximum deformation with a preferred orientation trending ≈140° (with respect to the horizontal axis).

The restored surface using the meridian paleomagnetic reference data is almost perfect. Its rectangular shape nearly matches the original (shape coefficient = 1.6%), the spatial distribution of dilation values is close to the theoretical one (although smaller), and the trend of the deformation ellipse is similar in the regions of maximum deformation. We are certainly able to predict the deformation tendency by unfolding the surface with this paleomagnetic dataset. Unfortunately, however, this success is not

Fig. 5. The computer model: undevelopable cone. A) Definition of the folded surface: undevelopable cone with paleomagnetic vectors (obtained from the developable one). B) Theoretical deformation (expected dilation and deformation ellipse) calculated by comparing the restored developable cone with the folded surface. C) Restoration of the surface using paleomagnetic vectors (before and after the optimization process) and without considering the paleomagnetic vector (equivalent to the UNFOLD method by Gratier and Guillier, 1993).

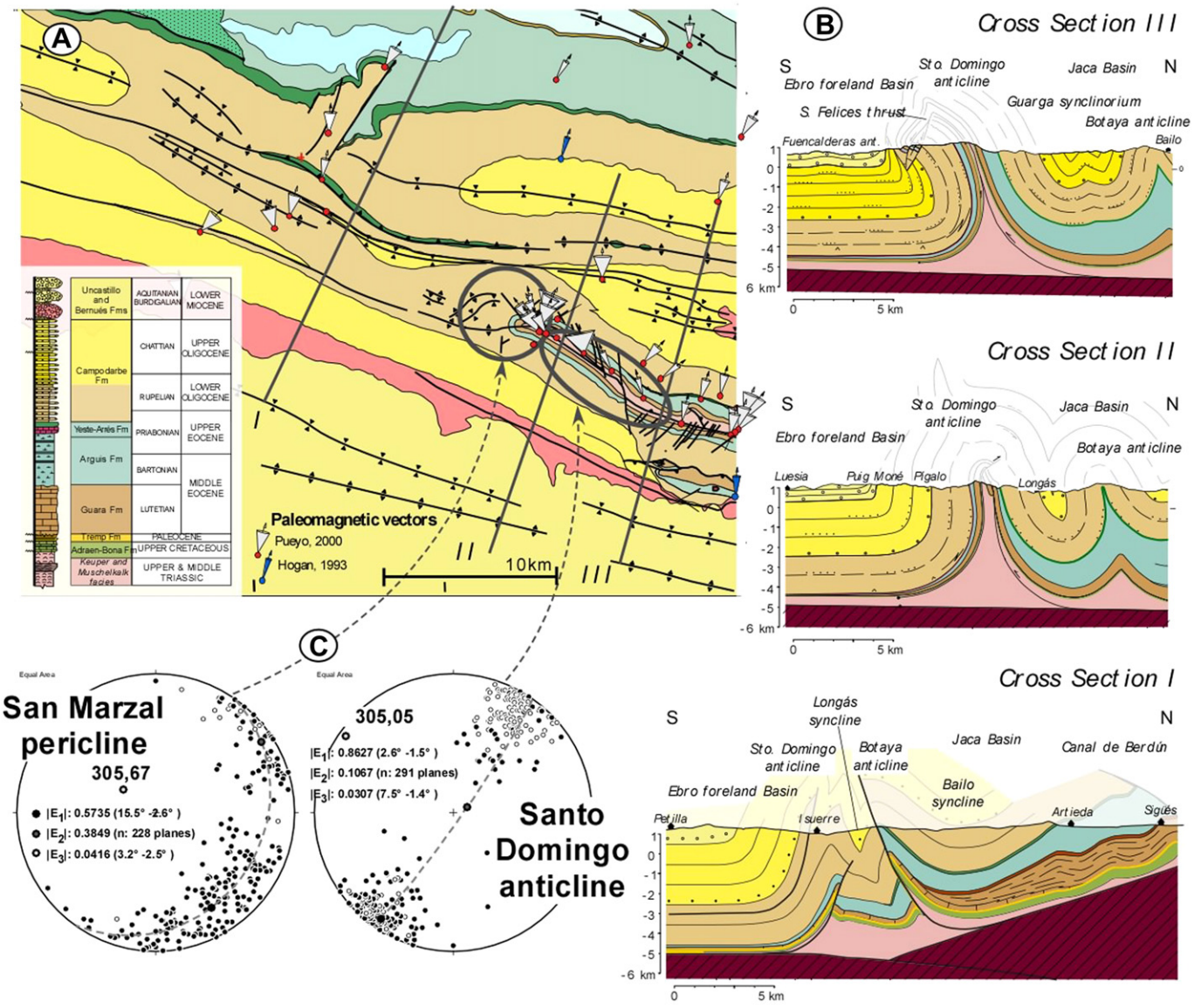

Fig. 7. Geological setting of the Sto. Domingo anticline at the western end of the south Pyrenean sole thrust. A) Geological sketch map displaying the location of paleomagnetic data and cross-sections (modified from Puigdefábregas, 1975, Millan, 1996, 2006 and Pueyo, 2000). B) Balanced cross sections; Isuerre (Oliva et al., 1996, 2011) and San Marzal (Millán, 1996, 2006). Note the effect of the fold axis plunge (cone generator trend) on the geometry of the pre-Campodarbe sequence. C) Stereographic projection of bedding poles; San Marzal pericline and Sto Domingo anticline. A cylindrical best-fit (Bingham's [1974] statistics) performed with the Stereonet program characterizes the fold trend and plunge.

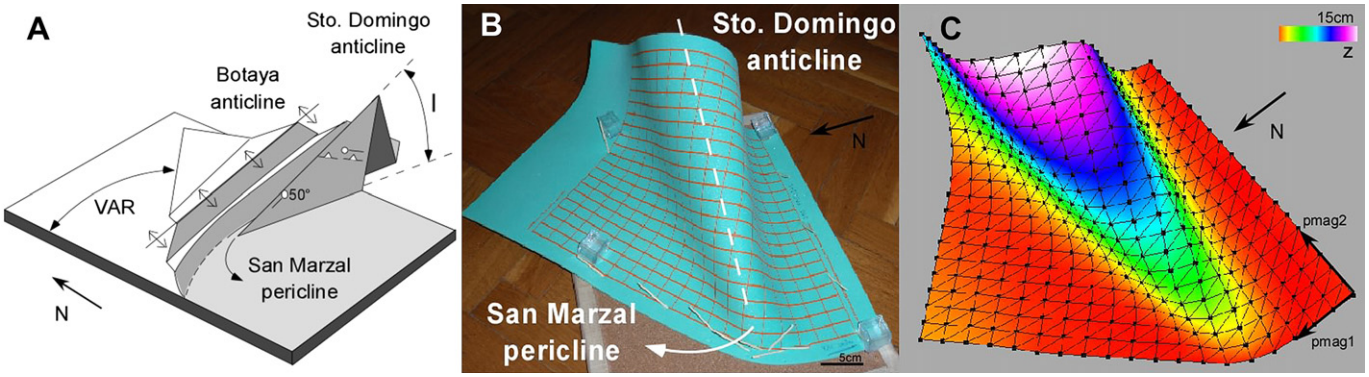

Fig. 8. Analog modelling of the San Marzal pericline. A) Simple paper cut-out model of the San Marzal pericline (Millán et al., 1992). B) EVA foam model on which lines parallel and perpendicular to the paleomagnetic reference vector have been screen-printed. D) Final 3D reconstruction of the model (gOcad) with the z coordinate displayed.

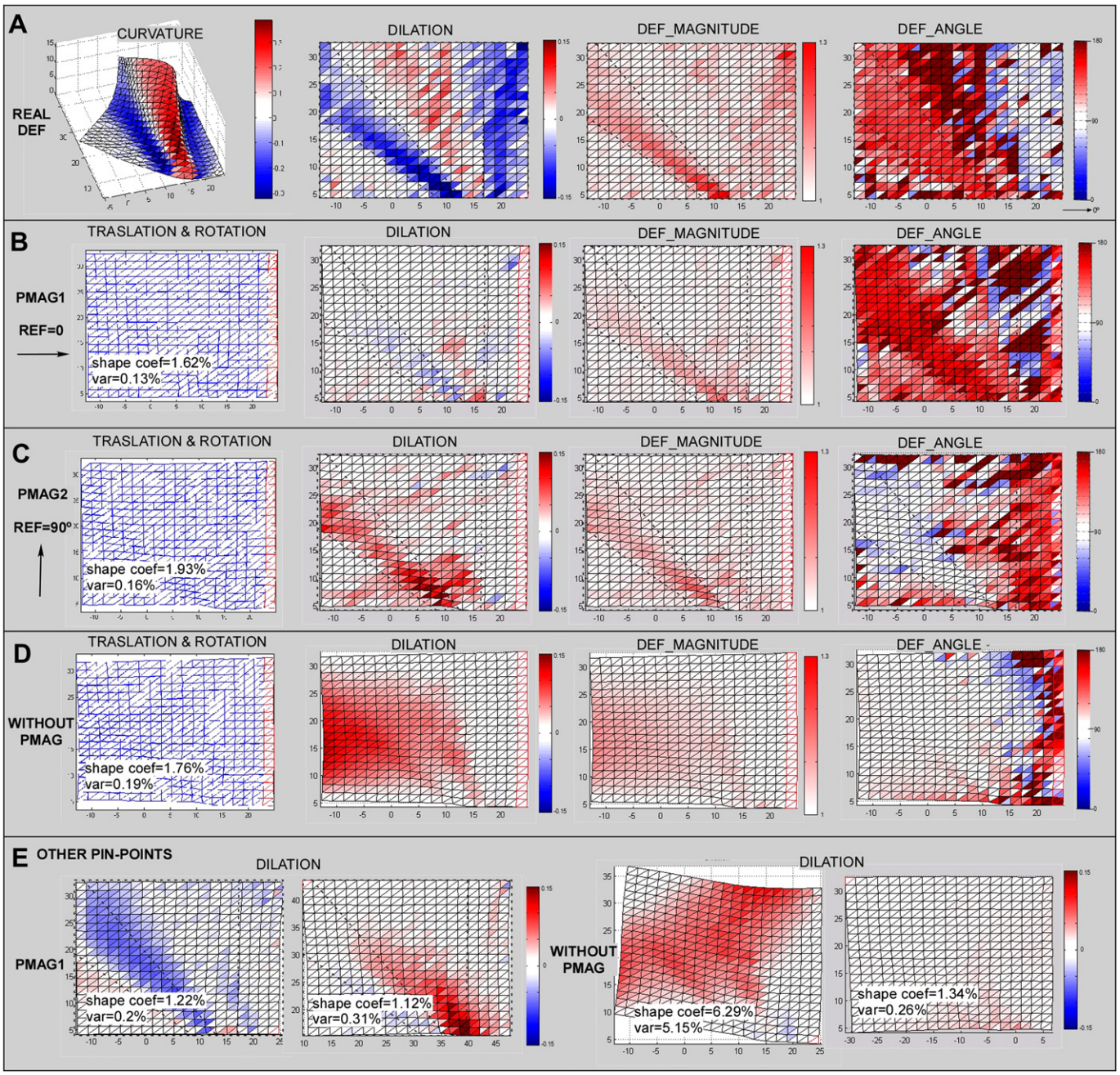

Fig. 9. Analog model restoration. A) Simple curvature of the folded surface. Theoretical (expected) dilation and deformation ellipse. B) Restoration with pmag1 (meridian lineation): restored surface after the translation/rotation and iterating steps and after the welding step (before optimization): dilation and deformation ellipse. The shape coefficient and its variance are also calculated. The pin-line is located on the eastern side (red triangles) C) Restoration with pmag2 (parallel lineation). D) Restoration without paleomagnetic data. E) Restoration using different pin-points (red triangles): with pmag1 and without pmag.

generalized. The restored surface using the parallel reference leads to similar deformation areas but with the opposite sign. In any case, the restored surfaces fit the expected result much better when paleomagnetic data are considered in the restoration than when they are not. Specifically, when paleomagnetic data are not used, the deformation propagates toward the opposite side of the pin-line.

In this experiment, we selected the initial pin-line with geological criteria. It is the fixed reference line used to anchor the model and to start unfolding the surface. In the San Marzal analog model, this line is located to the south of the structure and it represents an undeformed and non-rotated portion of the Ebro foreland Basin. We have also experimented with other starting points to test the effect of this variable. The first simulation (Fig. 9E) uses the pin-point in the lower right corner of the surface, which still holds some physical meaning. The restoration with paleomagnetism locates a deformation area close to the real one, but slightly displaced upwards (eastwards) where there is no anchor. In this case, the restoration without paleomagnetism does not make geological sense: it is far from the expected rectangular initial shape of the surface (shape coefficient = 6.3%), and indicates an inconsistent pattern of deformation. The second simulation fixes the pin-point to an active part of the surface during the deformation, the upper left corner (an absolutely meaningless

choice). The shape of the restored surface converges reasonably well with the expected one because the triangles can easily be rearranged with fewer restrictions. On the other hand, the internal deformation cannot be accurately located. Once again, in terms of deformation, the restoration of the same example without using paleomagnetic vectors leads to results which are geologically meaningless.

4. Conclusions

In this paper, we present a new surface restoration method. It is based on the combined use of the bedding plane and paleomagnetic vector to relate deformed and undeformed surfaces in non-cylindrical structures.

The method is applied to two examples: the computer model of a deformed cone (undevelopable), and a 3D reconstruction of an analog model inspired by the conical ending of the Santo Domingo anticline (Southern Pyrenees). Accurate knowledge of the deformed and undeformed surfaces is the main advantage of using this type of analog model, and enables us to quantify the goodness of fit of our restoration method.

The method using paleomagnetic data works better than the equivalent that only considers the bedding plane as a reference in several respects:

1. It may help locate the strain and its anisotropy. In the examples studied, the restoration algorithm was more efficient in delimiting regions of expected deformation.
2. Although in most cases the deformation areas are similar to the surface curvature patterns, the restored surface gives more information about anisotropy and preferential orientation of the deformation than curvature analysis.
3. The paleomagnetism reference vector restricts rotation and thus anchors the surface to more than one point (not just the pin-line). This leads to the surface having a more coherent and constant shape, not so dependent on the pin-line, which must in any case be chosen by geological criteria.

The method also shows some weakness and flaws that should be considered in future developments:

1. The distribution and quality of paleomagnetic vectors across the folded surface influence the results. Therefore, the paleomagnetic dataset must be accurate and reliable, including densely spaced measurements that are evenly distributed across the studied structures.
2. Pinpointing the factors that determine the deformation path of a restored surface is a challenging task and is not always possible. There are two main reasons: a poor reconstruction (a non-developable surface or inaccurate paleomagnetic data) or actual surface strain. When deformation propagates to the opposite side of the pin-line, we know that this is caused by the restoration method itself. On the other hand, if the deformation is coherent when unfolding the surface from different sides, we should study the resulting deformation carefully since this may contain relevant geological information.
3. The optimization process does not help with the process of identifying zones of deformation because it distributes errors that are likely to contain information.

Acknowledgments

The research was funded by grants for the following projects: Pmag3Drest (CGL-2006-2289-BTE, CGL2009-14214) and TIN2007-66423 from the Spanish Ministry of Science, 3DR3 & GeoPyrDatabases (PI165/09 & CTPP01/07) and T48 research group from the Government of Aragon and ESF, and the INTERREG III (EU)-CTP programme respectively. In addition, MJRO receives funding (PTA2007-0282) from the Spanish Ministry of Science. Stereographic projections were made using the "Stereonet" program (4.5.9) developed by Richard Allmendinger to whom we are very grateful. We want also to acknowledge the contribution of the reviewers, Pauline Durand and Peter Cobbold, whose comments have helped us improve the manuscript.

References

Arenas, C., Millán, H., Pardo, G., Pocoví, A., 2001. Ebro Basin continental sedimentation associated with late compresional pyrenean tectonics (NE Iberia): controls on margin fans and alluvial systems. Basin Research 13, 65–89.

Arriagada, C., 2004. Rotations tectoniques et déformation de l'avant arc des Andes centrales au cours du Cénozoïque. Mémoires de Géosciences-Rennes 107, 1–308.

Arriagad, C., Roperch, P., Mpodozis, C., Cobbold, P., 2008. Paleogene building of the Bolivian Orocline: tectonic restoration of the central Andes in 2-D map view. Tectonics 27.

Audiber, M., 1991. Déformation Discontinue et Rotations de Blocs, Méthodes Numériques de Restauration, Mém. Doc. Cent. Armoricain Etud. Struc. Socles, vol. 40, p. 239, Géosci, Rennes, Rennes, France.

Bonhommet, N., Cobbold, P.R., Perroud, H., Richardson, A., 1981. Paleomagnetism and cross-folding in a key area of the Asturian Arc (Spain). Journal of Geophysical Research 86, 1873–1887.

Bingham, C., 1974. An antipodally symmetric distribution on the sphere. Annals of Statistics 2, 1201–1225.

Bourgeois, O., Cobbold, P.R., Rouby, D., Thomas, J.C., Shein, V., 1997. Least squares restoration of Tertiary thrust sheets in map view, Tajik Depression, Central Asia. Journal of Geophysical Research B, Solid Earth and Planets 102 (12), 27553–27573.

Buddin, T.S., Kane, S.J., Williams, G.D., Egan, S.S., 1997. A sensitivity analysis of 3-dimensional restoration techniques using vertical and inclined shear constructions. Tectonophysics 269 (1–2), 33–50.

Cobbold, P.R., Percevault, M.N., 1983. Spatial integration of strains using finite elements. Journal of Structural Geology 5, 299–305.

Cooper, M.A., 1983. The calculation of bulk strain in oblique and inclined balanced sections. Journal of Structural Geology 5 (2), 161–165.

Dahlstrom, C.D., 1969. Balanced cross sections. Canadian Journal Earth Sciences 6, 743–757.

Delaunay, B., 1934. Sur la sphère vide. Bulletin of the Academy of Sciences of the U.S.S.R., Classe des Sciences Mathématiques et Naturelle 7 (6), 793–800.

Dunbar, J.A., Cook, R.W., 2003. Palinspastic reconstruction of structure maps: an automated finite element approach with heterogeneous strain. Journal of Structural Geology 26, 1021–1036.

Durand-Riard, P., Caumon, G., Muron, P., 2010. Balanced restoration of geological volumes with relaxing meshing constraints. Computer and Geosciences 36 (4), 441–452.

Elliott, D., 1976. The energy balance and deformation mechanisms of thrust sheets. Philosophical Transactions of the Royal Society A283, 289–312.

Fernández, O., Muñoz, J.A., Arbués, P., 2003. Quantifying and correcting errors derived from apparent dip in the construction of dip-domain cross-sections. Journal of Structural Geology 25, 35–42.

Fisher, R.A., 1953. Dispersion on a sphere. Proceedings of the Royal Society of London. Series A 217, 295–305.

Fischer, M., Keating, D., 2004. Photogrammetric techniques for analyzing displacement, strain, and structural geometry in physical models: application to the growth of monoclinal basement uplifts. Geological Society of America Journal.

Goguel, J., 1952. Traité de tectonique. Comptes Rendus Critiques, Paris, Masson, in-8°, 383 p. (translated in 1962 as Tectonics [San Francisco, Freeman, 384p]. by H.E. Thalman).

Gratier, J.P., Guillier, B., Delorme, A., Odonne, F., 1991. Restoration and balance of a folded and faulted surface by best-fitting of finite elements; principle and applications. Journal of Structural Geology 13 (1), 111–115.

Gratier, J.P., Guiller, B., 1993. Compatibility constraints on folded and faulted strata and calculation of total displacement using computational restoration (UNFOLD program). Journal of Structural Geology 15, 391–402.

Griffiths, P., Jones, S., Salter, N., Schaefer, F., Osfield, R., Reiser, R., 2002. A new technique for 3D-flexural-slip restoration. Journal of Structural Geology 24, 733–782.

Guzofski, C., Mueller, J., Shaw, J., Muron, P., Medwedeff, D., Bilotti, F., Rivero, C., 2009. Insights into the mechanisms of fault-related folding provided by volumetric structural restorations using spatially varying mechanical constraints. American Association of Petroleum Geologists Bulletin 93, 479–502.

Hjelle, Ø, Dæhlen, M., 2006. Triangulations and applications. In: Farin, G., Hege, H.C., Hoffman, D., Johnson, C.R., Polthier, K., Rumpf, M. (Eds.), Mathematics and Visualization. Springer, Berlin, p. 234.

Hossack, J.R., 1979. The use of balanced cross-sections in the calculation of orogenic contraction: a review. Journal of the Geological Society of London 136, 705–711.
Kerr, H.G., White, N., Brun, J.P., 1993. An automatic method for determining three-dimensional normal fault geometries. Journal of Geophysical Research 98, 17837–17857.
Kirkpatrick, S., Gelatt, C.D., Vecchi, M.P., 1983. Optimization by simulated annealing. Science. New Series 220 (4598), 671–680.
Lanaja, J.M., 1987. Contribución de la exploración petrolífera al conocimiento de la Geología de España. Inst. Geol. Mine, España, Ed.). p. 465, 17 mapas.
Leger, M., Thibaut, M., Gratier, J.P., Morvan, J.M., 1997. A least-squares method for multisurface unfolding. Journal of Structural Geology 19 (5), 735–743.
Maerten, L., Maerten, F., 2006. Chronologic modelling of faulted and fractured reservoirs using geomechanically based restoration: technique and industry applications. AAPG Bulletin 90 (8), 1201–1226.
Massot, J., 2002. Implémentation de méthodes de restauration équilibrée 3D (implementation of 3D balanced restoration methods). Ph.D. Dissertation, Institut Polytechnique National de Lorraine, Nancy, France, p. 157.
McCaig, A.M., McClelland, E., 1992. Palaeomagnetic techniques applied to thrust belts. In: McClay, K.R. (Ed.), Thrust Tectonics. Chapman y Hall Eds., London, pp. 209–216, p. 447.
McElroy, R., 1990. Thrust kinematics and syntectonic sedimentation: the Pyrenean frontal ramp, Huesca, Spain. Unpublished PhD thesis, University of Cambridge, p. 175.
Millán, H., 1996. Estructura y cinemática del frente de cabalgamiento surpirenaico en las Sierras Exteriores Aragonesas. Tesis Doctoral Universidad de Zaragoza, p. 330.
Millán, H., 2006. Estructura y cinemática del frente de cabalgamiento surpirenaico en las Sierras Exteriores aragonesas. Colección de Estudios Altoaragoneses, vol. 53. Instituto de Estdios Altoaragoneses, Huesca, ISBN 84-8127-165-9, p. 398.
Millán, H., Parés, J.M., Pocoví, A., 1992. Modelización sencilla de la estructura del sector occidental de las sierras marginales aragonesas (Prepirineo, provincias de Huesca y Zaragoza). III Congreso Geol. España. Simposios 2, 140–149.
Millán, H., Pocoví, A., Casas, A., 1995. El frente de cabalgamiento surpirenaico en el extremo occidental de las Sierras Exteriores: sistemas imbricados y pliegues de despegue. Revista de la Sociedad Geológica de España 8 (1–2), 73–90.
Moretti, I., Lepage, F., Guiton, M., 2005. KINE3D: a new 3D restoration method based on a mixed approach linking geometry and geomechanics. Oils & Gas Science and Technology (Rev IFP) 60, 1–12.
Moretti, I., 2008. Working in complex areas: new restoration workflow based on quality control, 2D and 3D restorations. Marine and Petroleum Geology 25, 205–218.
Muron, 2005. Méthodes numériques 3-D de restauration des structures géologiques faillées. PhD École Nationale Supérieure de Géologie, Institut National Polytechnique de Lorraine.
Nichols, G.J., 1984. Thrust tectonics and alluvial sedimentation, Aragón, Spain. Unpublished PhD Darwin College, University of Cambridge, p. 243.
Nichols, G.J., 1987. The structure and stratigraphy of the Western External Sierras of the Pyrenees, Northern Spain. Geological Journal 22 (3), 245–259.
Oliva, B., 2000. Estructura y cinemática del frente surpirenaico en el sector central de la cuenca de Jaca-Pamplona. MSc thesis. Universidad de Zaragoza, p. 100.
Oliva, B., Pueyo, E.L., 2007. Gradient of shortening and vertical-axis rotations in the Southern Pyrenees (Spain), insights from a synthesis of paleomagnetic data. Revista de la Sociedad Geológica de España 20 (1–2), 105–118.
Oliva, B., Millán, H., Pocoví, A., Casas, A.M., 1996. Estructura de la Cuenca de Jaca en el sector occidental de las Sierras Exteriores Aragonesas. Geogaceta 20 (4), 800–802.
Oliva, B., Casas, A.M., Pueyo, E.L., Pocoví, A., 2011. Structural and paleomagnetic evidence for non-rotational kinematics in the western termination of the External Sierras (southwestern central Pyrenees). Geologica Acta (in press)
Press, W., Flannery, B., Teukolsky, S., Vetterling, W., 1992. Numerical Recipes in C: The Art of Scientific Computing, Chapter 10.9 Simulated Annealing pp. 450–455.
Pueyo, E.L., 1994. Estudio magnetotectónico preliminar de las Sierras Exteriores Altoaragonesas. MSc thesis. Universidad de Zaragoza, p. 155.
Pueyo, E.L., 2000. Rotaciones paleomagnéticas en sistemas de pliegues y cabalgamientos. Tipos, causas, significado y aplicaciones (ejemplos del Pirineo Aragonés). PhD thesis, Universidad de Zaragoza, p. 296.
Pueyo, E.L., 2010. Evaluating the paleomagnetic reliability in fold and thrust belt studies. Trabajos de Geología 30 (1), 145–154.
Pueyo, E.L., Parés, J.M., Millán, H., Pocoví, A., 2003. Conical folds and apparent rotations in paleomagnetism (A case study in the Pyrenees). Tectonophysics 362 (1/4), 345–366.
Pueyo, E.L., Pocoví, A., Millán, H., Sussman, A.J., 2004. Map view model to correct and calculate shortening in rotated thrust fronts using paleomagnetic data. In: Sussman, A.J., Well, A.B. (Eds.), Paleomagnetic and Structural Analyses of Orogenic Curvature, vol. 383. Geological Society of America Spec. Publ, pp. 57–71.
Puigdefábregas, C., 1975. La sedimentación molásica en la cuenca de Jaca. Pirineos 104, 1–188.
Ramsay, J.G., 1967. Folding and Fracturing of Rocks. McGraw Hill, New York, p. 568.
Ramsay, J.G., Huber, M.I., 1983. The Techniques of Modern Structural Geology. In: Strain Analysis, vol. 1. Academic Press, London, p. 307.
Rouby, D., Cobbold, P.R., Szatmari, P., Demercian, S., Coelho, D., Rici, J.A., 1993. Restoration in plan view of faulted Upper Cretaceous and Oligocene horizons and its bearing on the history of salt tectonics in the Campos Basin (Brazil). Tectonophysics 228, 435–445.
Rouby, D., Suppe, J., Xiao, H., 2000. 3D restoration of complexly faulted and folded surfaces using multiple unfolding mechanisms. American Association of Petroleum Geologists 84, 805–829.
Suppe, J., 1985. Principles of Structural Geology. Prentice-Hall Inc., Englewood Cliffs, N.J, p. 537.
Sussman, A.J., Chase, C.G., Pueyo, E.L., Mitra, G., Weil, A., 2011. The impact of vertical-axis rotations on shortening estimates. Earth and Planetary Sciences Letters (in review)
Thibert, B., Gratier, J.P., Morvan, J.M., 2005. A direct method for modelling and unfolding developable surfaces and its application to the Ventura Basin (California). Journal of Structural Geology 27, 303–316.
Turner, J.P., 1990. Structural and stratigrafic evolution of the West Jaca thrust-top basin, Spanish Pyrenees. Journal of the Geological Society of the London 147, 177–184.
Van der Voo, R., 1990. The reliability of paleomagnetic data. Tectonophysics 184, 1–9.
Williams, G.D., Kane, S., Buddin, T.S., Richards, A.J., 1997. Restoration and balance of complex folded and faulted rock volumes; flexural flattening, jigsaw fitting and decompaction in three dimensions. Tectonophysics 273 (3–4), 203–218.